Available online at www.sciencedirect.com
ScienceDirect
Chinese Journal of Aeronautics 21(2008) 550-558
Chinese Journal of Aeronautics
www.elsevier.com/locate/cja

Aircraft Flutter Modal Parameter Identification Using a Numerically Robust Least-squares Estimator in Frequency Domain

Tang Wei*, **Shi Zhongke**, **Chen Jie**

College of Automation, Northwestern Polytechnical University, Xi'an 710072,China

Received 20 June 2008; accepted 26 September 2008

Abstract

Recently, frequency-based least-squares (LS) estimators have found wide application in identifying aircraft flutter parameters. However, the frequency methods are often known to suffer from numerical difficulties when identifying a continuous-time model, especially, of broader frequency or higher order. In this article, a numerically robust LS estimator based on vector orthogonal polynomial is proposed to solve the numerical problem of multivariable systems and applied to the flutter testing. The key idea of this method is to represent the frequency response function (FRF) matrix by a right matrix fraction description (RMFD) model, and expand the numerator and denominator polynomial matrices on a vector orthogonal basis. As a result, a perfect numerical condition (numerical condition equals 1) can be obtained for linear LS estimator. Finally, this method is verified by flutter test of a wing model in a wind tunnel and real flight flutter test of an aircraft. The results are compared to those with notably LMS PolyMAX, which is not troubled by the numerical problem as it is established in *z* domain (e.g. derived from a discrete-time model). The verification has evidenced that this method, apart from overcoming the numerical problem, yields the results comparable to those acquired with LMS PolyMAX, or even considerably better at some frequency bands.

Keywords: flutter; modal parameter; parameter identification; LS estimator; numerically robust; ill-conditioned

1 Introduction

As an aeroelastic phenomenon, aircraft fluttering results from the coactions of three sorts of forces—aerodynamic, elastic, and inertial forces within a sufficiently short stretch of time, which leads to an unstable oscillation, and even more serious, to a catastrophic structural failure[1].

In order to prevent such a disaster from happening, a flutter test is always required in design and acceptance of an airplane[2-3]. The test usually includes identification of its modal parameters from testing data, and prediction of the critical point of flutter through tracking damping ratio in the subcritical state. Obviously, an accurate and reliable estimation of modal parameters is essential for flutter prediction.

Several system identification methods have found wide application in flutter testing in both frequency and time domains[4]. Recently, a frequency domain least-squares (LS) estimator has been developed to estimate flutter modal parameters[5]. It can improve the accuracy of modal parameters estimation when dealing with noisy data. However, the frequency methods are known with a poor numerical conditioning when identifying a continuous-time model, especially, of broader frequency

*Corresponding author. Tel.: 86-29-88431323.
E-mail address: tangwei@nwpu.edu.cn
Foundation items: Aeronautical Science Foundation of China (2007ZD53053); NPU Foundation for Fundamental Research (NPU-FFR-W018104)

(more than 2 decades) or higher order (more than 20). This numerical problem worsens both the modeling performance and the model order selection capability.

Several attempts have been made in the past to eliminate numerical degeneracy in the frequency domain identification. They range from an appropriate scaling of frequency[6-7] to the decomposition of the numerator and denominator of the model equation on a separate base of orthogonal polynomials[7-8]. Apart from imposing more limits on bandwidth and complexity, these efforts could not solve the numerical problems thoroughly.

This article proposes a numerically robust frequency-based estimator for flutter modal parameter identification, which uses vector orthogonal polynomials to solve the numerical condition problem. Ref.[9] introduced the vector orthogonal polynomials and applied them to single input single output (SISO) systems. This article attempts to extend this method to multivariable systems, and apply it to flutter modal parameter identification. Section 3 provides a detailed description of the algorithm. Finally, the method is verified by the test data from a wind tunnel and real flight test.

2 Problem Formulations

Fig.1 depicts the simplified schema of the flutter test. The test typically consists of measurements of the excitation applied to the structure and the response to the excitation. The aircraft aeroelastic system in a flutter test can be regarded as a linear dynamic system. The measured spectrum data are input $\boldsymbol{U}$ and output $\boldsymbol{Y}$ disturbed with noise. $\boldsymbol{U}_0$, $\boldsymbol{Y}_0$ are the exact value of measurements, respectively. $\boldsymbol{M}_U$, $\boldsymbol{M}_Y$ are the measured noise in input and output, respectively. $\boldsymbol{N}_\mathrm{E}$ denotes the unmeasured excitation, such as atmospheric turbulence or airflow.

The measurements $\boldsymbol{U}$ and $\boldsymbol{Y}$ are related to the exact values $\boldsymbol{U}_0$ and $\boldsymbol{Y}_0$ through

$$\boldsymbol{U}(\mathrm{j}\omega_k)=\boldsymbol{U}_0(\mathrm{j}\omega_k)+\boldsymbol{N}_U(\mathrm{j}\omega_k)=\boldsymbol{U}_0(\mathrm{j}\omega_k)+\boldsymbol{M}_U(\mathrm{j}\omega_k) \tag{1}$$

$$\boldsymbol{Y}(\mathrm{j}\omega_k)=\boldsymbol{Y}_0(\mathrm{j}\omega_k)+\boldsymbol{N}_Y(\mathrm{j}\omega_k)=\boldsymbol{Y}_0(\mathrm{j}\omega_k)+\boldsymbol{M}_Y(\mathrm{j}\omega_k)+\boldsymbol{H}_0(\mathrm{j}\omega_k)\boldsymbol{N}_\mathrm{E}(\mathrm{j}\omega_k) \tag{2}$$

where $\boldsymbol{H}(\mathrm{j}\omega_k)$ denotes the frequency response function (FRF) between the accelerometer output and the true excitation input at discrete Fourier transform (DFT) frequency ω_k ($k=1,2,\cdots,N$, the number of frequency lines), $\boldsymbol{H}_0(\mathrm{j}\omega_k)$ is the FRF from accelerometer response to atmospheric turbulence. $\boldsymbol{N}_U$, $\boldsymbol{N}_Y$ denote the noise in input and output, respectively. During analyzing the experiment model, the process noise $\boldsymbol{H}_0(\mathrm{j}\omega_k)\boldsymbol{N}_\mathrm{E}(\mathrm{j}\omega_k)$ is considered to be undesirable.

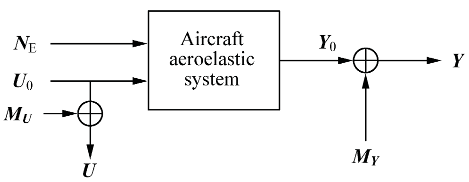

Fig.1 A simplified model of flight flutter test.

By use of an errors-in-variables (EIV) stochastic noise model, the measured input/output (I/O) Fourier data can be represented by

$$\boldsymbol{Z}(\mathrm{j}\omega_k)=\boldsymbol{Z}_0(\mathrm{j}\omega_k)+\Delta\boldsymbol{Z}(\mathrm{j}\omega_k) \tag{3}$$

where $\boldsymbol{Z}=[\boldsymbol{U}^\mathrm{T}(\mathrm{j}\omega_k)\quad \boldsymbol{Y}^\mathrm{T}(\mathrm{j}\omega_k)]^\mathrm{T}$, $\boldsymbol{Z}_0=[\boldsymbol{U}_0^\mathrm{T}(\mathrm{j}\omega_k)\quad \boldsymbol{Y}_0^\mathrm{T}(\mathrm{j}\omega_k)]^\mathrm{T}$, $\Delta\boldsymbol{Z}=[\boldsymbol{N}_U^\mathrm{T}(\mathrm{j}\omega_k)\quad \boldsymbol{N}_Y^\mathrm{T}(\mathrm{j}\omega_k)]^\mathrm{T}$.

Since in practice, the Fourier spectra are calculated via a DFT, we can assume $\Delta\boldsymbol{Z}(\mathrm{j}\omega_k)$ is a zero mean, complex normally distributed vector with the following covariance matrix

$$E(\Delta\boldsymbol{Z}(\mathrm{j}\omega_k)\Delta\boldsymbol{Z}^\mathrm{H}(\mathrm{j}\omega_k))=\boldsymbol{C}_Z(\mathrm{j}\omega_k)=\begin{bmatrix}\boldsymbol{C}_U^2(\mathrm{j}\omega_k) & \boldsymbol{C}_{UY}^2(\mathrm{j}\omega_k)\\ \boldsymbol{C}_{YU}^2(\mathrm{j}\omega_k) & \boldsymbol{C}_Y^2(\mathrm{j}\omega_k)\end{bmatrix} \tag{4}$$

where $\boldsymbol{C}_U(\mathrm{j}\omega_k)$ and $\boldsymbol{C}_Y(\mathrm{j}\omega_k)$ denote the input and output noise covariance respectively, and $\boldsymbol{C}_{UY}(\mathrm{j}\omega_k)$ and $\boldsymbol{C}_{YU}(\mathrm{j}\omega_k)$ denote the input-output and output-input noise covariance, respectively.

3 Theoretical Aspects

3.1 Parametric model

The flutter test is of a typical multiple input multiple output (MIMO) system, the relationship between outputs and inputs can be modeled in the frequency domain by means of a right matrix fraction description (RMFD) given by

$$\boldsymbol{H}(\mathrm{j}\omega_k)=\boldsymbol{B}(s_k)\boldsymbol{A}^{-1}(s_k) \tag{5}$$

where $\boldsymbol{H}(\mathrm{j}\omega_k)\in\mathbf{C}^{N_\mathrm{o}\times N_\mathrm{i}}$ is the FRF. The matrix polynomials $\boldsymbol{A}(s_k)\in\mathbf{C}^{N_\mathrm{i}\times N_\mathrm{i}}$ and $\boldsymbol{B}(s_k)\in\mathbf{C}^{N_\mathrm{o}\times N_\mathrm{i}}$ are defined by

$$\boldsymbol{A}(s_k)=\sum_{j=0}^{n_\mathrm{a}}\boldsymbol{A}_j s_k^j\ ,\quad \boldsymbol{B}(s_k)=\sum_{j=0}^{n_\mathrm{b}}\boldsymbol{B}_j s_k^j$$

where $\boldsymbol{A}_j\in\mathbf{C}^{N_\mathrm{i}\times N_\mathrm{i}}$, $\boldsymbol{B}_j\in\mathbf{C}^{N_\mathrm{o}\times N_\mathrm{i}}$, $s_k=\mathrm{j}\omega_k$, $k=1,2,\cdots,N$. The matrix coefficients $\boldsymbol{A}_j$ and $\boldsymbol{B}_j$ are the parameters to be estimated. The practical flutter system is a causal system, in which, for simplicity, it is reasonable to assume that $n_\mathrm{a}=n_\mathrm{b}=n$.

3.2 Weighted least-squares (WLS) estimator

Using Eq.(5), the relationship between the oth outputs $(o=1,2,\cdots,N_\mathrm{o})$ and inputs is given by

$$\boldsymbol{H}_o(\mathrm{j}\omega_k)=\boldsymbol{B}_o(s_k)\boldsymbol{A}^{-1}(s_k) \tag{6}$$

where $\boldsymbol{H}_o(\mathrm{j}\omega_k)$ is the oth row of the FRF $\boldsymbol{H}(\mathrm{j}\omega_k)$ and $\boldsymbol{B}_o(s_k)\in\mathbf{C}^{1\times N_\mathrm{i}}$ is the oth row-vector of numerator polynomial matrix $\boldsymbol{B}(s_k)$. Similar to $\boldsymbol{B}(s_k)$, $\boldsymbol{B}_o(s_k)$ is defined as

$$\boldsymbol{B}_o(s_k)=\sum_{j=0}^{n}\boldsymbol{B}_{oj}s_k^j$$

By replacing the model $\boldsymbol{H}_o(\mathrm{j}\omega_k)$ by the multiplication of measured FRF $\hat{\boldsymbol{H}}_o(\mathrm{j}\omega_k)$ and the denominator polynomial $\boldsymbol{A}(s_k)$, the linearized (weighted) error equation becomes

$$\boldsymbol{E}_o(\mathrm{j}\omega_k)=W_o(\hat{\boldsymbol{H}}_o(\mathrm{j}\omega_k)\boldsymbol{A}(s_k)-\boldsymbol{B}_o(s_k))\approx\boldsymbol{0} \tag{7}$$

where W_o is an additional scalar frequency-weighting for each output.

The relationship given by Eq.(7) exists at each output, which can be formulated as $\boldsymbol{J\theta}\approx\boldsymbol{0}$

$$\begin{bmatrix}\boldsymbol{\Gamma}_1 & \boldsymbol{0} & \cdots & \boldsymbol{0} & \boldsymbol{\Psi}_1\\ \boldsymbol{0} & \boldsymbol{\Gamma}_2 & \cdots & \boldsymbol{0} & \boldsymbol{\Psi}_2\\ \vdots & \vdots & \ddots & \vdots & \vdots\\ \boldsymbol{0} & \boldsymbol{0} & \boldsymbol{0} & \boldsymbol{\Gamma}_{N_\mathrm{o}} & \boldsymbol{\Psi}_{N_\mathrm{o}}\end{bmatrix}\begin{bmatrix}\boldsymbol{\theta}_{\boldsymbol{B}_1}\\ \boldsymbol{\theta}_{\boldsymbol{B}_2}\\ \vdots\\ \boldsymbol{\theta}_{\boldsymbol{B}_{N_\mathrm{o}}}\\ \boldsymbol{\theta}_{\boldsymbol{A}}\end{bmatrix}\approx\boldsymbol{0} \tag{8}$$

with

$$\boldsymbol{\Gamma}_o=\begin{bmatrix}W_o(\mathrm{j}\omega_1)[1\quad s_1\quad\cdots\quad s_1^n]\\ W_o(\mathrm{j}\omega_2)[1\quad s_2\quad\cdots\quad s_2^n]\\ \vdots\\ W_o(\mathrm{j}\omega_N)[1\quad s_N\quad\cdots\quad s_N^n]\end{bmatrix}$$

$$\boldsymbol{\Psi}_o=\begin{bmatrix}W_o(\mathrm{j}\omega_1)[1\quad s_1\quad\cdots\quad s_1^n]\otimes\hat{\boldsymbol{H}}(\mathrm{j}\omega_1)\\ W_o(\mathrm{j}\omega_2)[1\quad s_2\quad\cdots\quad s_2^n]\otimes\hat{\boldsymbol{H}}(\mathrm{j}\omega_2)\\ \vdots\\ W_o(\mathrm{j}\omega_N)[1\quad s_N\quad\cdots\quad s_N^n]\otimes\hat{\boldsymbol{H}}(\mathrm{j}\omega_N)\end{bmatrix}$$

$$\boldsymbol{\theta}_{\boldsymbol{B}_o}=[\boldsymbol{B}_{o0}^\mathrm{T}\quad \boldsymbol{B}_{o1}^\mathrm{T}\quad\cdots\quad \boldsymbol{B}_{on}^\mathrm{T}]^\mathrm{T}$$

$$\boldsymbol{\theta}_{\boldsymbol{A}}=[\boldsymbol{A}_0\quad \boldsymbol{A}_1\quad\cdots\quad \boldsymbol{A}_n]^\mathrm{T}$$

where $\otimes$ denotes the kronecker product. In practice, the so called normal equation $\boldsymbol{J}^\mathrm{H}\boldsymbol{J\theta}=\boldsymbol{0}$ is commonly used, which leads to a more compact formulation and a reduction of computation time.

However, in the case of continuous time models, ill-conditioned Jacobian and normal matrix will lower the numerical precision of LS estimator. To overcome this defect, the orthogonal polynomials or frequency scaling has been introduced, but neither of the methods is easily applicable to MIMO system.

3.3 LS estimator based on orthogonal polynomials

This section puts forward a numerically robust LS estimator for MIMO system, which solves the numerical condition problem on the base of vector orthogonal polynomials.

The equation errors of all outputs are

$$\boldsymbol{E}(s_k)=[\boldsymbol{E}_1^\mathrm{H}(s_k)\quad \boldsymbol{E}_2^\mathrm{H}(s_k)\quad\cdots\quad \boldsymbol{E}_{N_\mathrm{o}}^\mathrm{H}(s_k)]^\mathrm{H}\approx\boldsymbol{0}$$

According to Eq.(7), $\boldsymbol{E}(s_k)$ can be written as

$$\boldsymbol{E}(s_k)=\boldsymbol{W}_\mathrm{E}[\boldsymbol{H}(\mathrm{j}\omega_k)\quad -\boldsymbol{I}][\boldsymbol{A}(s_k)\quad \boldsymbol{B}(s_k)]^\mathrm{T} \tag{9}$$

where $\boldsymbol{W}_\mathrm{E}=\mathrm{diag}(\boldsymbol{W}_1,\boldsymbol{W}_2,\cdots,\boldsymbol{W}_{N_\mathrm{o}})$ is a diagonal weighting matrix.

The weighted linear LS problem can be settled by minimizing the cost function given by

$$V=\sum_{o=1}^{N_\mathrm{o}}\sum_{k=1}^{N}\boldsymbol{E}_o(s_k)\boldsymbol{E}_o^\mathrm{H}(s_k)=\sum_{o=1}^{N_\mathrm{o}}\sum_{k=1}^{N}\mathrm{vec}(\boldsymbol{E}_o(s_k))^\mathrm{H}\bullet \mathrm{vec}(\boldsymbol{E}_o(s_k))=\sum_{k=1}^{N}\boldsymbol{R}^\mathrm{H}\boldsymbol{R} \tag{10}$$

with

$$\boldsymbol{R}=\begin{bmatrix}\mathrm{vec}(\boldsymbol{E}_1)\\ \mathrm{vec}(\boldsymbol{E}_2)\\ \vdots\\ \mathrm{vec}(\boldsymbol{E}_{N_\mathrm{o}})\end{bmatrix}=\mathrm{vec}[\boldsymbol{E}_1\quad \boldsymbol{E}_2\quad\cdots\quad \boldsymbol{E}_{N_\mathrm{o}}]=\mathrm{vec}(\boldsymbol{E}^\mathrm{T})=$$

$$\mathrm{vec}\left([\boldsymbol{A}^{\mathrm{T}}(s_k) \quad \boldsymbol{B}^{\mathrm{T}}(s_k)] \begin{bmatrix} \hat{\boldsymbol{H}}^{\mathrm{T}}(\mathrm{j}\omega_k) \\ -\boldsymbol{I} \end{bmatrix} \boldsymbol{W}_{\mathrm{E}} \right) \tag{11}$$

where $\mathrm{vec}(\bullet)$ denotes the vectorization of the matrix formed by stacking the columns of matrix into a single column vector.

According to kronecker product property

$$\mathrm{vec}(\boldsymbol{JKL}) = (\boldsymbol{L}^{\mathrm{T}} \otimes \boldsymbol{J})\mathrm{vec}(\boldsymbol{K})$$

Eq.(11) becomes

$$\boldsymbol{R} = \left(\boldsymbol{W}_{\mathrm{E}}[\hat{\boldsymbol{H}}(\mathrm{j}\omega_k) \quad -\boldsymbol{I}] \otimes \boldsymbol{I} \right) \begin{bmatrix} \mathrm{vec}(\boldsymbol{A}^{\mathrm{T}}(s_k)) \\ \mathrm{vec}(\boldsymbol{B}^{\mathrm{T}}(s_k)) \end{bmatrix} \tag{12}$$

Defining vector polynomials

$$\boldsymbol{Q}(s_k) = \begin{bmatrix} \mathrm{vec}(\boldsymbol{A}^{\mathrm{T}}(s_k)) \\ \mathrm{vec}(\boldsymbol{B}^{\mathrm{T}}(s_k)) \end{bmatrix} \tag{13}$$

the corresponding cost function is

$$V = \boldsymbol{Q}^{\mathrm{H}}(s_k)\boldsymbol{W}_k^{\mathrm{H}}\boldsymbol{W}_k\boldsymbol{Q}(s_k) \tag{14}$$

and

$$\boldsymbol{W}_k = \left(\boldsymbol{W}_{\mathrm{E}}[\hat{\boldsymbol{H}}(\mathrm{j}\omega_k) \quad -\boldsymbol{I}] \otimes \boldsymbol{I} \right)$$

Clearly, Eq.(14) defines an inner product for the vector polynomials.

$$\langle \boldsymbol{Q}, \boldsymbol{R} \rangle_{\boldsymbol{W}} = \sum_{k=1}^{N} \boldsymbol{Q}^{\mathrm{H}}(s_k)\boldsymbol{W}_k^{\mathrm{H}}\boldsymbol{W}_k\boldsymbol{R}(s_k) \tag{15}$$

where $\boldsymbol{Q}(s_k)$, $\boldsymbol{R}(s_k)$ are $(N_{\mathrm{i}}^2 + N_{\mathrm{o}}N_{\mathrm{i}})$ dimensional vector polynomials. Therefore, in this setting, a polynomial vector $\boldsymbol{Q}(s_k)$ should be found to have minimal cost function V with a strict degree n. To fix the problem uniquely, the last element of the parameter vectors $\boldsymbol{\theta}$, $\boldsymbol{A}_n$ is fixed to unit matrix. Of course, another option is permissible, for example, by choosing $\boldsymbol{B}_n = \boldsymbol{I}$.

To solve the question, we expand $\boldsymbol{Q}(s_k)$ based on the orthogonal vector

$$\boldsymbol{Q}(s_k) = \sum_{i=0}^{n} \boldsymbol{P}_i(s_k)\boldsymbol{\lambda}_i \tag{16}$$

and

$$\boldsymbol{\lambda}_i = [\lambda_{1,i} \quad \lambda_{2,i} \quad \cdots \quad \lambda_{(N_{\mathrm{i}}^2+N_{\mathrm{o}}N_{\mathrm{i}}),i}]^{\mathrm{T}} \tag{17}$$

where $\boldsymbol{\lambda}_i$ denotes the "weights", and $\boldsymbol{P}_i(s_k)$ is the polynomial orthogonal matrix in terms of

$$\langle \boldsymbol{P}_{\mathrm{k}}, \boldsymbol{P}_{\mathrm{l}} \rangle_{\boldsymbol{W}} = \delta_{\mathrm{kl}}\boldsymbol{I}$$

With Eq.(16), the LS equation error $\boldsymbol{E}(s_k) \approx \boldsymbol{0}$ now becomes

$$\boldsymbol{W\Phi X} = \boldsymbol{0} \tag{18}$$

where $\boldsymbol{W} = \mathrm{diag}(\boldsymbol{W}_1, \boldsymbol{W}_2, \cdots, \boldsymbol{W}_N)$, $\boldsymbol{X} = [\boldsymbol{\lambda}_1^{\mathrm{T}} \quad \boldsymbol{\lambda}_2^{\mathrm{T}} \quad \cdots \quad \boldsymbol{\lambda}_n^{\mathrm{T}}]$, $\boldsymbol{\Phi} = \begin{bmatrix} \boldsymbol{P}_0(s_1) & \cdots & \boldsymbol{P}_n(s_1) \\ \vdots & & \vdots \\ \boldsymbol{P}_0(s_N) & \cdots & \boldsymbol{P}_n(s_N) \end{bmatrix}$.

The orthogonality of $\boldsymbol{P}_i(s_k)$ implies that $\boldsymbol{\Phi}^{\mathrm{H}} \bullet \boldsymbol{W}^{\mathrm{H}}\boldsymbol{W\Phi} = \boldsymbol{I}$. Hence, the LS equation is best conditioned (condition number=1).

The optimization problem is now reduced to

$$\min V = \min \sum_{k=1}^{N} \boldsymbol{Q}^{\mathrm{H}}(s_k)\boldsymbol{W}_k^{\mathrm{H}}\boldsymbol{W}_k^{\mathrm{H}}\boldsymbol{Q}(s_k) = \min \boldsymbol{X}^{\mathrm{H}}\boldsymbol{\Phi}^{\mathrm{H}}\boldsymbol{W}^{\mathrm{H}}\boldsymbol{W\Phi X} = \min \boldsymbol{X}^{\mathrm{H}}\boldsymbol{X} = \min \sum_{i=1}^{n} (\lambda_{1,i}^2 + \lambda_{2,i}^2 + \cdots + \lambda_{(N_{\mathrm{i}}^2+N_{\mathrm{o}}N_{\mathrm{i}}),i}^2) \tag{19}$$

where $\boldsymbol{A}(s_k)$ should be regarded as being monic. In order to minimize the cost function, let $\boldsymbol{\lambda}_0 = \boldsymbol{\lambda}_1 = \cdots = \boldsymbol{\lambda}_{n-1} = \boldsymbol{0}$, which minimizes Eq.(19) into

$$\min (\lambda_{1,n}^2 + \lambda_{2,n}^2 + \cdots + \lambda_{(N_{\mathrm{i}}^2+N_{\mathrm{o}}N_{\mathrm{i}}),n}^2) \tag{20}$$

and thus

$$\boldsymbol{Q}(s_k) = \boldsymbol{P}_n\boldsymbol{\lambda}_n = \boldsymbol{P}_n \begin{bmatrix} \lambda_{1,n} \\ \lambda_{2,n} \\ \vdots \\ \lambda_{(N_{\mathrm{i}}^2+N_{\mathrm{o}}N_{\mathrm{i}}),n} \end{bmatrix} \tag{21}$$

It is known that the highest degree coefficient matrix of $\boldsymbol{P}_n$ is upper triangular[14]

$$\boldsymbol{P}_n = \left[\begin{array}{cccc|ccc} p_{11} & p_{12} & \cdots & p_{1,N_{\mathrm{i}}^2} & p_{1,(N_{\mathrm{i}}^2+1)} & \cdots & p_{1,(N_{\mathrm{i}}^2+N_{\mathrm{o}}N_{\mathrm{i}})} \\ & p_{22} & \cdots & p_{2,N_{\mathrm{i}}^2} & p_{2,(N_{\mathrm{i}}^2+1)} & \cdots & p_{2,(N_{\mathrm{i}}^2+N_{\mathrm{o}}N_{\mathrm{i}})} \\ & & \ddots & \vdots & \vdots & & \vdots \\ & & & p_{N_{\mathrm{i}}^2,N_{\mathrm{i}}^2} & p_{N_{\mathrm{i}}^2,(N_{\mathrm{i}}^2+1)} & \cdots & p_{N_{\mathrm{i}}^2,(N_{\mathrm{i}}^2+N_{\mathrm{o}}N_{\mathrm{i}})} \\ \hline & & & & p_{(N_{\mathrm{i}}^2+1),(N_{\mathrm{i}}^2+1)} & \cdots & p_{(N_{\mathrm{i}}^2+1),(N_{\mathrm{i}}^2+N_{\mathrm{o}}N_{\mathrm{i}})} \\ & & & & & \ddots & \vdots \\ & & & & & & p_{(N_{\mathrm{i}}^2+N_{\mathrm{o}}N_{\mathrm{i}}),(N_{\mathrm{i}}^2+N_{\mathrm{o}}N_{\mathrm{i}})} \end{array} \right] s_k^n + \cdots \tag{22}$$

Using Eqs.(21)-(22), can be obtained

$$\boldsymbol{Q}(s_k)=\left[\begin{array}{cccc:ccc} p_{11} & p_{12} & \cdots & p_{1,N_\mathrm{i}^2} & p_{1,(N_\mathrm{i}^2+1)} & \cdots & p_{1,(N_\mathrm{i}^2+N_\mathrm{o}N_\mathrm{i})} \\ & p_{22} & \cdots & p_{2,N_\mathrm{i}^2} & p_{2,(N_\mathrm{i}^2+1)} & \cdots & p_{2,(N_\mathrm{i}^2+N_\mathrm{o}N_\mathrm{i})} \\ & & \ddots & \vdots & \vdots & & \vdots \\ & & & p_{N_\mathrm{i}^2,N_\mathrm{i}^2} & p_{N_\mathrm{i}^2,(N_\mathrm{i}^2+1)} & \cdots & p_{N_\mathrm{i}^2,(N_\mathrm{i}^2+N_\mathrm{o}N_\mathrm{i})} \\ \hdashline & & & & p_{(N_\mathrm{i}^2+1),(N_\mathrm{i}^2+1)} & \cdots & p_{(N_\mathrm{i}^2+1),(N_\mathrm{i}^2+N_\mathrm{o}N_\mathrm{i})} \\ & & & & & \ddots & \vdots \\ & & & & & & p_{(N_\mathrm{i}^2+N_\mathrm{o}N_\mathrm{i}),(N_\mathrm{i}^2+N_\mathrm{o}N_\mathrm{i})} \end{array}\right]\left[\begin{array}{c} \lambda_{1,n} \\ \vdots \\ \lambda_{N_\mathrm{i}^2,n} \\ \hdashline \lambda_{(N_\mathrm{i}^2+1),n} \\ \vdots \\ \lambda_{(N_\mathrm{i}^2+N_\mathrm{o}N_\mathrm{i}),n} \end{array}\right]s_k^n+\cdots=$$

$$\left[\begin{array}{c:c} \boldsymbol{P}_{11} & \boldsymbol{P}_{12} \\ \hdashline \boldsymbol{0} & \boldsymbol{P}_{22} \end{array}\right]\left[\begin{array}{c} \boldsymbol{\alpha} \\ \hline \boldsymbol{\beta} \end{array}\right]s_k^n+\cdots \tag{23}$$

where $\boldsymbol{P}_{11}$, $\boldsymbol{P}_{12}$, $\boldsymbol{P}_{22}$ are block matrices.

To normalize the solution, $\boldsymbol{A}(s_k)$ is required to be monic, therefore,

$$\boldsymbol{Q}(s_k)=\begin{bmatrix} \mathrm{vec}(\boldsymbol{A}^\mathrm{T}(s_k)) \\ \mathrm{vec}(\boldsymbol{B}^\mathrm{T}(s_k)) \end{bmatrix}=\begin{bmatrix} \mathrm{vec}(\boldsymbol{I}_{N_\mathrm{i}^2}) \\ \times \\ \vdots \\ \times \end{bmatrix}s_k^n+\cdots \tag{24}$$

and

$$\begin{bmatrix} \mathrm{vec}(\boldsymbol{I}_{N_\mathrm{o}^2}) \\ \times \\ \vdots \\ \times \end{bmatrix}=\left[\begin{array}{c:c} \boldsymbol{P}_{11} & \boldsymbol{P}_{12} \\ \hdashline \boldsymbol{0} & \boldsymbol{P}_{22} \end{array}\right]\left[\begin{array}{c} \boldsymbol{\alpha} \\ \hline \boldsymbol{\beta} \end{array}\right] \tag{25}$$

The values of "×" need not be specified for the moment. From Eq.(25), the cost function can be decreased by letting $\boldsymbol{\beta}$ to equal zero, and $\boldsymbol{\alpha}=\boldsymbol{P}_{11}^{-1}\mathrm{vec}(\boldsymbol{I}_{N_\mathrm{i}^2})$ to meet the normalized condition. The solution of LS estimator is

$$\boldsymbol{Q}(s_k)=\boldsymbol{P}_n\boldsymbol{\lambda}_n=\boldsymbol{P}_n\begin{bmatrix} \boldsymbol{P}_{11}^{-1}\mathrm{vec}(\boldsymbol{I}_{N_\mathrm{i}^2}) \\ \boldsymbol{0} \end{bmatrix} \tag{26}$$

Obviously, how to construct the vector orthogonal basis is a very important for this approach. Owing to the limitation of space, more details would be omitted. Information about numerically stable and time-saving construction of vector orthogonal polynomial basis is available in Refs. [9-10].

4 Flutter Modal Parameters Identification

4.1 Data preparation for identification

Fig.2 depicts the typical setup of the flutter test. It is equipped with a flutter excitation system (FES), which is operated to add programmed digital signals such as sweeps to the control system actuator commands for structural excitation. The responses are measured by accelerometers located in the aircraft nose, vertical and horizontal tails, and wingtips.

In practice, the input signal for excitation is known beforehand and is free of noise. For simplicity, only the errors in the output will be considered. As a result, the measured frequency response $\hat{\boldsymbol{H}}(\mathrm{j}\omega_k)$ is estimated by H_1 estimator

$$\hat{\boldsymbol{H}}(\mathrm{j}\omega_k)=\boldsymbol{S}_{\boldsymbol{YU}}(\mathrm{j}\omega_k)\boldsymbol{S}_{\boldsymbol{UU}}^{-1}(\mathrm{j}\omega_k)$$

where $\boldsymbol{S}_{\boldsymbol{YU}}(\mathrm{j}\omega_k)$ and $\boldsymbol{S}_{\boldsymbol{UU}}(\mathrm{j}\omega_k)$ are respectively the cross spectrum and auto spectrum of the input $\boldsymbol{U}$ and output $\boldsymbol{Y}$.

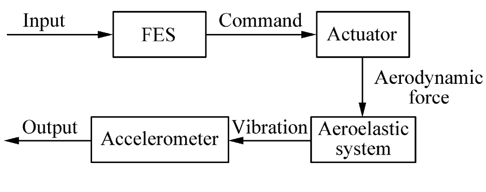

Fig.2 Flutter test schematic diagram.

4.2 Weighting

An adequate choice of the frequency dependent weighting function W_o in Eq.(7) can improve the quality of the parameter estimates. The so called iterative quadratic maximum likelihood (IQML)[11] estimator based on the scalar weighting

$$W_o^m(\mathrm{j}\omega_k)=\mathrm{tr}((\boldsymbol{A}^{m-1}(s_k))^\mathrm{H}\boldsymbol{C}_{\boldsymbol{H}_o}(\mathrm{j}\omega_k)\boldsymbol{A}^{m-1}(s_k))^{-1/2}$$

is used to improve the efficiency of the LS estimates.

$\mathrm{tr}(\bullet)$ is the trace operator, $(\bullet)^m$ is the mth iteration, $\boldsymbol{C}_{\boldsymbol{H}_o}$ is the covariance of $\boldsymbol{H}_o$. At every iteration step, the weighting should be updated using the calculated denominator of the previous step.

Similar to the method developed by C. K. Sanathanan and J. Koerner[12], a developed iterative procedure is adopted to improve the estimates. It is observed that in the case of sufficiently high signal-to-noise ratios, the cost function of the IQML converges to the maximum likelihood (ML) cost function[13], although the estimator is inconsistent.

4.3 Deriving modal parameters

Let $p_r (r = 1, 2, \cdots, n)$ be the poles of the transfer function, then the corresponding modal frequency and damping ratio can be obtained as

$$\left.\begin{aligned} f_r &= \frac{\mathrm{Im}(p_r)}{2\pi} \\ \zeta_r &= -\frac{\mathrm{Re}(p_r)}{|p_r|} \end{aligned}\right\} \tag{27}$$

where $\mathrm{Im}(\bullet)$ and $\mathrm{Re}(\bullet)$ denote imaginary and real parts of the complex, respectively. The poles p_r can be found from the denominator polynomial coefficients $\boldsymbol{A}_j$. The companion matrix $\boldsymbol{A}_{\mathrm{c}}$, made up of the coefficients, is given by[14]

$$\boldsymbol{A}_{\mathrm{c}} = \begin{bmatrix} \boldsymbol{A}'_{n-1} & \cdots & \boldsymbol{A}'_1 & \boldsymbol{A}'_0 \\ \boldsymbol{I} & & \boldsymbol{0} & \boldsymbol{0} \\ & \ddots & & \vdots \\ \boldsymbol{0} & & \boldsymbol{I} & \boldsymbol{0} \end{bmatrix}$$

where $\boldsymbol{A}'_j = -\boldsymbol{A}_n^{-1}\boldsymbol{A}_j$. The poles p_r are given by the eigenvalues of $\boldsymbol{A}_{\mathrm{c}}$. Obviously, the modal parameters are derived from the matrix coefficients, and the attention will be focused on estimating the coefficients of FRF.

5 Experiment Study

5.1 Wind tunnel test

A schematic layout of the wind tunnel test is shown in Fig.3. All tests were performed in a low-speed wind tunnel. A rectangular wing model with a trailing edge flap was mounted horizontally in the wind tunnel. The flutter mounting system consisted of a moving plate supported by a system of four circular rods and a centered flat-plate strut.

An electrical motor installed on the lower surface of the moving plate was used to drive the trailing edge flap. The flap was connected to the motor by a shaft. The electromotor had an encoder to measure the actual angular position of the flap. The vibration of aeroelastic system was measured by four accelerometers mounted in each corner of the wing. The flutter testing was similar to that introduced in Ref.[15].

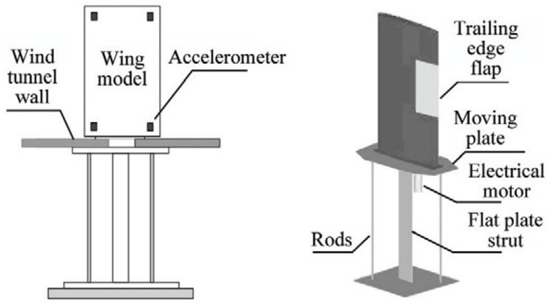

Fig.3 Schematic layout of the wind tunnel test system.

In the wind tunnel test, the air force produced by trailing edge flap was used to excite the wing model. The input signals in these tests were at the trailing edge position and the output signal was the acceleration measured in the wing model.

Digital signals were generated and sent to the trailing edge flap as input, and the responses measured by accelerometers were recorded. In the experiments, the linear sweep signals (chirp signals) were employed for excitation. This kind of inputs made it possible to distinguish frequencies ranging from 1 Hz to 10 Hz when running tests. The sample frequency for data acquisition was 256 Hz.

Figs.4-5 depict examples of input and output signals measured in one of the wind tunnel tests. Fig. 4 depicts the input flap deflection in degrees. It represents a linear sweep generated signal to the flap angle. Fig.5 shows a response of one accelerometer. Fig.6 shows the FRFs for parameter identification, which were derived from all accelerometers in the tests.

The proposed numerically robust frequency-domain LS estimator was applied to data analysis. As a current standard tool in industry, the LMS PolyMax[16] method is also adopted for reference. Fig.7 shows the stabilization diagrams for numerically robust LS estimator method while Fig.8 shows for the PolyMax method. In these figures, the crosses represent the identified frequency location of the poles related to the model order indicated on the vertical axis. Since the two stabilization diagrams are similar, the results provided by the numerically robust LS estimator are considerably clearer in comparison with the PolyMAX, especially in the vicinity of 7 Hz.

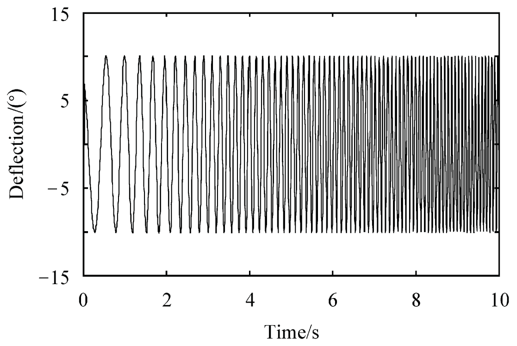

Fig.4 Deflection of flap (linear sweep input).

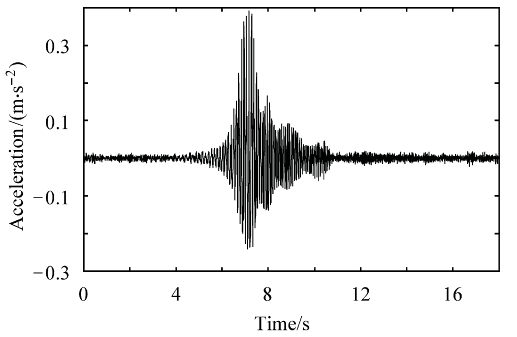

Fig.5 Measured noisy response of an accelerometer.

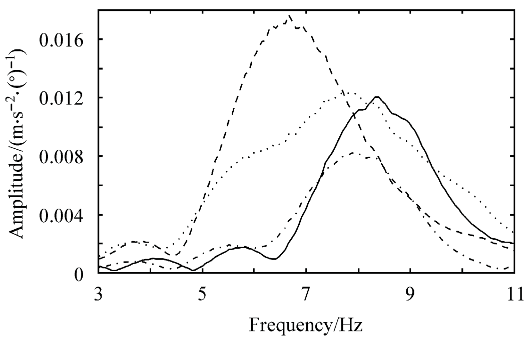

Fig.6 FRFs for four accelerometers mounted in each corner of the wing.

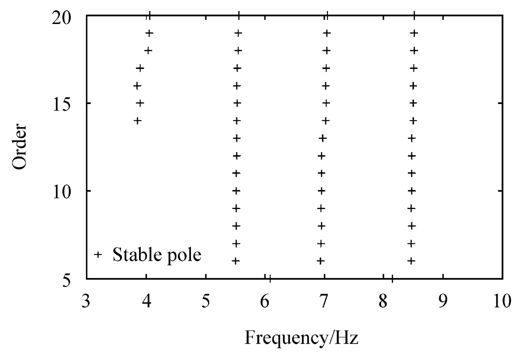

Fig.7 Stabilization diagram obtained from numerically robust LS estimator.

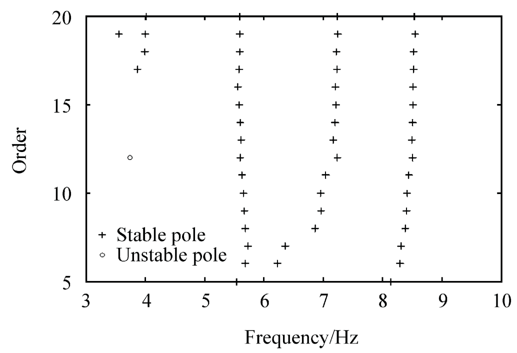

Fig.8 Stabilization diagram obtained from PolyMAX.

Table 1 lists some results in illustration of experimental data. The comparison of the identification results shows that numerically robust LS estimator can eliminate numerical degeneracy and yield results similar to those with PolyMAX.

Table 1 Comparison of the identification results between numerically robust LS estimator and PolyMAX

Mode	Numerically robust LS estimator		PolyMAX	
	Frequency/Hz	Dampling/%	Frequency/Hz	Dampling/%
1	4.06	4.40	4.01	4.15
2	5.61	2.61	5.56	2.90
3	7.11	1.94	7.18	2.16
4	8.58	3.43	8.62	3.30

5.2 Flight flutter test

This section intends to use real flight test to verify the effectiveness of the proposed algorithm. A large aircraft was excited by the outer aileron control signals with a sine sweep signal added in. As inputs, either the sine sweep generated signal or the angles at the control surfaces can be chosen, while the measured acceleration responses at various locations of the airplane: fuselage, engines, and wings are chosen as outputs. Data from 8 accelerometers were analyzed. As an example, Fig.9 shows the responses measured at the wing tip.

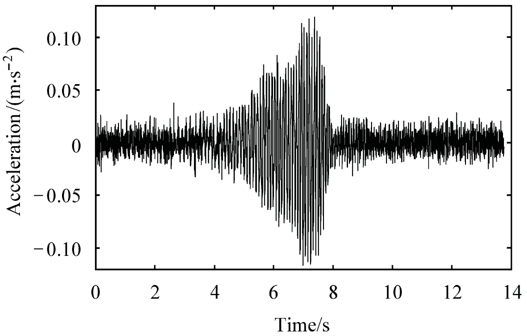

Fig.9 Measured responses from the accelerometer at the wing tip.

While the test is interrupted by the heavy noise, an efficacious data prefilter in time-frequency domain becomes indispensable[17-18]. Then, the LS estimator using clear data is implemented for modal parameters identification. As regards the numerical problem caused by the aeroelastic systems of high or moderate order, the numerically robust approach is implemented to model the measured FRFs with a RMFD form n=21. Fig.10 depicts one of the measured FRFs together with synthesized transfer function. For comparison, the estimation obtained from PolyMAX is also provided.

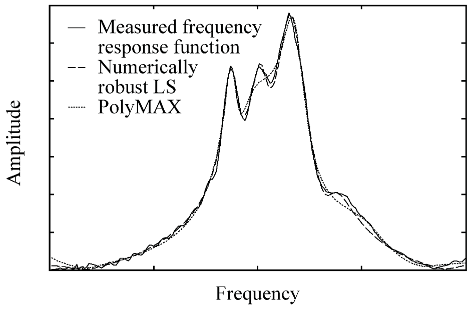

Fig.10 Comparison among measured response function, synthesized transfer function numerically robust LS estimator, and PolyMAX.

As observed from Fig.10, the numerically robust approach proposed by the article is able to accurately model the measured response function, especially the three lightly damping modes. Its performance is even superior to that of PolyMax. This is owing to the reasonable condition number and the "optimal" weighting updated by iteration, which improve the quality of the estimation. In contrast, PolyMax is a non-iterative approach with a larger condition number.

6 Conclusions

This article presents a numerically robust LS estimator for MIMO system and applies it to analysis of data from flutter tests. The numerical condition problem of LS estimator is solved perfectly with condition number equals 1 based on vector orthogonal polynomials. The real measurement results evidence that the proposed method is of great use in flutter modal parameters identification.

References

[1] Wright J R. Flight flutter testing, lecture series on flutter of winged aircraft. Belgium: Von Karman Institute, 1991.

[2] Brenner M J, Lind R C, Voracek D F. Overview of recent flight flutter testing research at NASA Dryden. NASA CR 4792, 1997.

[3] Kehoe W M. A historical overview of flight flutter testing. NASA CR 4720, 1995.

[4] Cooper J E. Parameter estimation methods for flight flutter testing. Proceedings of the 80th AGARD Structures and Materials Panel, AGARD CP-566. 1995.

[5] Verboven P, Cauberghe B, Guillaume P, et al. Modal parameter estimation and monitoring for on-line flight flutter analysis. Mechanical Systems and Signal Processing 2004; 18(3): 587-610.

[6] Pintelon R, Kollar I. On the frequency scaling in continuous-time modeling. IEEE Transactions on Instrumentation and Measurement 2005; 54(1): 318-321.

[7] Pintelon R, Schoukens J. System identification: a frequency domain approach. Los Alamitos: IEEE Press, 2001.

[8] Rolain Y, Pintelon R, Xu K Q, et al. On the use of orthogonal polynomials in high order frequency domain system identification and its application to modal parameter estimation. Proceedings of the 33rd IEEE Conference on Decision and Control. 1994; 3365-3373.

[9] Bultheel A, van Barel M, Rolain Y, et al. Robust rational approxi-

mation for identification. Proceedings of the 40th IEEE Conference on Decision and Control. 2001; 4770- 4775.

[10] van Barel M, Bultheel A. A parallel algorithm for discrete least squares rational approximation. Numerische Mathematik 1992; 63(1): 99-121.

[11] Guillaume P, Pintelon R, Schoukens J. A weighted total least squares estimator for multivariable systems with nearly maximum likelihood properties. IEEE Transactions on Instrumentation and Measurement 1998; 47(4): 818-822.

[12] Sanathanan C K, Koerner J. Transfer function synthesis as a ratio of two complex polynomials. IEEE Transactions on Automatic Control 1963; 8(1): 56-58.

[13] Pintelon R, Guillaume P, Rolain Y, et al. Parametric identification of transfer functions in the frequency domain—a survey. IEEE Transactions on Automatic Control 1994; 39(11): 2245-2260.

[14] Heylen W, Lammens S, Sas P. Modal analysis theory and testing. Belgium: Katholieke Universiteit Leuven, 1998.

[15] Rivera J A, Jr, Dansberry B E, Bennett J R, et al. NACA 0012 benchmark model experimental flutter results with unsteady pressure distributions. AIAA-92-2396, 1992.

[16] Peeters B, van der Auweraer H, Guillaume P, et al. The PolyMAX frequency-domain method: a new standard for modal parameter estimation. Shock and Vibration 2004; 11(3-4): 395-409.

[17] Feron E, Duchesne L, Turevskiy A, et al. Time-frequency analysis for transfer function estimation and application to flutter clearance. Journal of Guidance, Control, and Dynamics 1998, 21(3); 375-382.

[18] Tang W, Shi Z K, Li H C. Frequency-domian GTLS identification combined with time-frequency filtering for flight flutter modal parameter identification. Chinese Journal of Aeronautics 2006; 19(1): 44-51.

Biographies:

Tang Wei Born in 1977, He received his B.S., M.S. and Ph.D. from Northwestern Polytechnical University in 2000, 2003, and 2006, respectively. He is presently a teacher there. His main research interest is system identification and signal processing.
E-mail: tangwei@nwpu.edu.cn

Shi Zhongke Born in 1956, he received B.S., M.S. and Ph.D. from Northwestern Polytechnical University in 1981, 1988 and 1994, respectively. His main research interest is states and parameters estimation and robust control.
E-mail: zkeshi@nwpu.edu.cn

Chen Jie Born in 1982, he received B.S. and M.S. from Northwestern Polytechnical University in 2004 and 2007, respectively. His research field is flight control.
E-mail: shuimujie@mail.nwpu.edu.cn